CHEMISTRY OF MATERIALS

ARTICLE

pubs.acs.org/cm

Self-Assembled and Cross-Linked Fullerene Interlayer on Titanium Oxide for Highly Efficient Inverted Polymer Solar Cells

Yen-Ju Cheng,* Fong-Yi Cao, Wei-Cheng Lin, Chiu-Hsiang Chen, and Chao-Hsiang Hsieh

Department of Applied Chemistry, National Chiao Tung University, 1001 Ta Hsueh Road, Hsin-Chu, 30010 Taiwan

Supporting Information

ABSTRACT: We have successfully designed and synthesized two oxetane-functionalized fullerene derivatives, [6,6]-phenyl-C_{61}-butyric oxetane ester (PCBO) and [6,6]-phenyl-C_{61}-butyric oxetane dendron ester (PCBOD). We demonstrated that the oxetane functionality with neutral nature can anchor onto the TiO_x surface via cationic ring-opening reaction under thermal and UV treatment, as evidenced by contact angle measurement and X-ray photoelectron spectroscopy. The self-assembly of PCBO, functionalized with one oxetane group, on the TiO_x surface forms an adhesive monolayer with intimate contact. Inverted bulk-heterojunction device B [ITO/TiO_x/SA-PCBO/P3HT:PCBM (1:1 w/w)/MoO_3/Ag, where ITO is indium tin oxide, SA is self-assembled, P3HT is poly(3-hexylthiophene), and PCBM is [6,6]-phenyl-C_{61}-butyric acid methyl ester] with this self-assembled PCBO (SA-PCBO) modifier showed an impressive power conversion efficiency (PCE) of 4.1%, which outperforms the reference device A (PCE = 3.6%) without this monolayer [ITO/TiO_x/P3HT:PCBM (1:1 w/w)/MoO_3/Ag]. This SA-PCBO modifier exerts multipositive effects on the interface, including improvement of exciton dissociation efficiency, reduction of charge recombination, decrease of the interface contact resistance, and passivation of the surface electron traps at the interface of TiO_x. Furthermore, PCBOD, containing two oxetane groups, is capable of self-assembling on the TiO_x surface and simultaneously undergoing cross-linking, generating a dense, robust, and pinhole-free multimolecular interlayer to further strengthen the interface characteristics. Device C [ITO/TiO_x/C-PCBOD/P3HT:PCBM(1:1, in wt%)/MoO_3/Ag] incorporating this cross-linked PCBOD (C-PCBOD) interlayer delivered the highest PCE of 4.5% which represents 26% enhancement over device A. This simple and easy strategy smartly integrates the advantages of self-assembly and cross-linking in a single fullerene-based molecule, showing promise in producing highly efficient inverted PSCs.

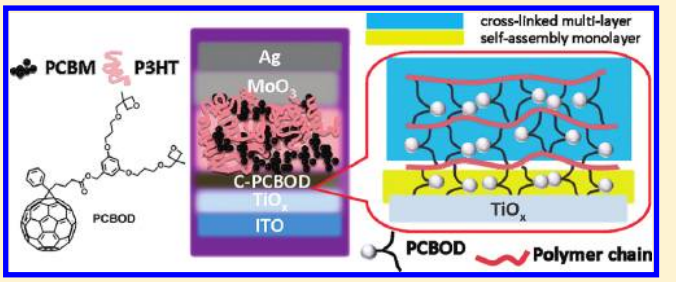

KEYWORDS: oxetane, self-assembled monolayer, cross-linking, inverted solar cells, titanium oxide

INTRODUCTION

Polymeric solar cells (PSCs) have emerged as a promising alternative technique for producing clean and renewable energy due to their potential for fabrication onto large areas of lightweight flexible substrates by low-cost solution processing. To maximize the donor−acceptor heterojunction interfacial area for efficient exciton dissociation, mainstream PSC devices adopt the concept of a bulk heterojunction (BHJ), where an active layer contains a p-type donor and an n-type acceptor to form an interpenetrating nanoscale network.[1] A conventional BHJ PSC with an active layer sandwiched by a low-work-function aluminum cathode and a hole-conducting poly(3,4-ethylenedioxylenethiophene):poly(styrene sulfonic acid) (PEDOT:PSS) layer on top of an indium tin oxide (ITO) substrate is the most widely used and investigated device configuration. On the basis of this device architecture, high power-conversion efficiencies (PCEs) of ca. 4−5% have been achieved for a blend containing a regioregular poly(3-hexylthiophene) (P3HT) and a fullerene derivative, [6,6]-phenyl-C_{61}-butyric acid methyl ester (PCBM).[2] Along with high performance, long-term stability is a primary area of concern for PSCs. However, it is highly challenging to develop a PSC that can achieve a high PCE while maintaining good ambient stability of the device. Prolonged exposure to air rapidly reduces the performance of unencapsulated conventional devices. Rapid oxidation of the low-work-function metal cathode and etching of ITO by the acidic PEDOT:PSS layer are the most common reasons for instability in conventional unencapsulated devices. An effective approach to solve these problems, and improve device lifetime, is to fabricate inverted PSCs.[3] By reversing the polarity of charge collection in a regular cell, air-stable Ag combining with an adjacent PEDOT:PSS layer can substitute for air-sensitive Al as the anodic electrode for efficient hole collection. In such an inverted configuration, it is necessary to insert an inorganic metal oxide (TiO_x or ZnO) between ITO and the active layer to function as an electron-selective contact.[4] Despite dramatic improvement in the operational lifetime, inverted solar cells still suffer from a trade-off between stability and performance. Recently reported inverted devices based on P3HT/PCBM composite exhibited PCEs in the range of ca. 2−4%, which is inferior to that of regular solar cells. The relatively lower performance is

Received: November 11, 2010
Revised: January 30, 2011
Published: February 22, 2011

dx.doi.org/10.1021/cm1032404 | *Chem. Mater.* 2011, 23, 1512–1518

attributed to the unfavorable energetic and incompatible chemical interfaces. Moreover, surface hydroxyl groups on metal oxide are known to act as electron traps, which in turn deteriorates electrical properties at the interface between metal oxide and organic layers.[5] It is believed that interfacial modification by incorporating an additional n-type C_{60} interlayer between the inorganic metal oxide and the organic active layer might improve device performance by modulating the electronic and orbital interactions at the upper and lower interfaces.[6] The major obstacle to realizing such a multilayer inverted device by cost-effective solution processing is that the deposited fullerene interlayer must possess sufficient resistance against the organic solvent used in processing the sequential active layer to prevent interfacial erosion.[7]

Recently, C_{60} derivatives functionalized with an anchoring group (carboxylic acid or phosphonic acid) that can form a self-assembled monolayer (SAM) on the metal oxide surface have been successfully used to enhance the device characteristics.[8] Through the chemical reaction between the anchoring groups and the hydroxyl groups of metal oxide surfaces to form the corresponding ester linkages, the formation of SAM can not only provide a immobilized C_{60} modifier to overcome the interfacial erosion but also terminate the hydroxyl groups on the metal oxide surfaces, which are known to be surface traps. However, the major drawbacks for SAM formation are insufficient coverage at the molecular scale and probable desorption of the molecules during wet processing, creating localized defects in this interlayer.[9] Moreover, loading of SAM C_{60} modifier is highly dependent on processing conditions.[10]

To overcome the deficiency of SAM, a cross-linkable fullerene material, [6,6]-phenyl-C_{61}-butyric styryl dendron ester (PCBSD), that uses the styrene group as thermal cross-linker has been described.[11] The formation of a cross-linked PCBSD (C-PCBSD) allows a sequential active layer to be successfully deposited on top of this interlayer without causing interfacial erosion and realizes an inverted device by all-solution processing. The C-PCBSD interlayer containing multiple layers of PCBSD molecules guarantees that the upper active layer and the bottom ZnO layer can be fully separated. Mutual diffusion between the upper active layer and the bottom metal-oxide layer can be thus avoided. An inverted solar cell device based on an ITO/ZnO/C-PCBSD/P3HT:PCBM/PEDOT:PSS/Ag configuration achieves an enhanced PCE of 4.4% in comparison to a reference device (PCE = 3.5%) without this interlayer.[11]

By taking advantage of both self-assembly and cross-linking approaches to introduce a fullerene interlayer, development of a new cross-linkable fullerene derivative that is also capable of self-assembling onto metal oxide surface will be a superb strategy to further improve the interface characteristics. However, it is rather challenging to search for an ideal functional group that can not only chemically anchor at surface of metal oxides but also proceed intermolecular cross-linking. Although chlorosilane functionalities to form siloxane-based network can fulfill the requirement, its high reactivity toward moisture makes it difficult to prepare and handle in air.[12] Oxetane functional group has been extensively utilized as an efficient cross-linker for the applications of organic electronics.[13] We envisage that the oxetane moiety may act as a promising cross-linker that can potentially serve a dual purpose. Considering the function of cross-linking, oxetane has many advantages over styrene. Radical polymerization of styrene is inhibited in air and needs to be carried out in a glovebox, whereas cationic polymerization of oxetane is stable in air. Ring-opening polymerization process of oxetane features low volume shrinkage of the surface layer and excellent adhesion on a substrate. Hence, microcracks or defects in films can be avoided. On the other hand, it is reasonable to postulate that hydroxyl groups on metal oxide can also serve as nucleophiles to open the ring of protonated oxetane, thereby forming a monolayer modifier by covalent bonding.[14] More importantly, compared to typical carboxylic acid, phosphonic acid, or chlorosilane serving as anchoring groups for SAM, neutral oxetane does not have an acidic nature that may etch and degrade the surface of metal oxides or hydrolyze the SAM molecules on the surface.[15]

On the basis of these considerations, we have designed and synthesized a new PCBM-based n-type material, [6,6]-phenyl-C_{61}-butyric oxetane dendron ester (PCBOD), functionalized with a small dendron containing two oxetane groups as the cross-linkers. PCBOD simultaneously realizes self-assembly anchoring on the TiO_x surface and cross-linking to form a multimolecular interlayer. Integration of this cross-linked PCBOD (C-PCBOD) into the inverted solar cells as an interlayer has achieved superior device performance.

RESULTS AND DISCUSSION

Synthesis of the materials used in this study is shown in Scheme 1. Etherification of 3-hydroxymethyl-3-methyloxetane **1** with 1,3-dibromopropane **2** afforded compound **3**, which was allowed to react with 3,5-dihydroxybenzyl alcohol **4** to obtain a small dendron **5** containing two oxetane groups. In the presence of *N*,*N*′-dicyclohexylcarbodiimide (DCC) and 4-(dimethylamino)pyridine (DMAP), PCBOD was easily prepared by the esterification of **5** with [6,6]-phenyl-C_{61}-butyric acid (PCBA), which was obtained by hydrolysis of PCBM (Scheme 1).

The core structure of PCBOD is based on the most widely used n-type material, PCBM, so PCBOD is expected to inherit all the excellent electrical properties of its parent molecule. Meanwhile, for self-assembly study, the [6,6]-phenyl-C_{61}-butyric oxetane ester (PCBO) functionalized with only one oxetane was also prepared. Upon treatment with thionyl chloride, the carboxylic acid in PCBA was first converted into the acid chloride, followed by reaction with 3-hydroxymethyl-3-methyloxetane to yield PCBO.

From the DSC measurement, PCBOD exhibited a T_g at 59 °C without showing any exothermic transition, meaning that the oxetane groups in PCBOD are thermally inert. To induce cationic oxetane ring-opening polymerization, a catalytic amount of photoacid generator (PAG) is required to generate acidic protons upon UV irradiation. Infrared spectroscopy was employed to monitor the transformation of functional groups during the cross-linking of PCBOD. The pristine PCBOD exhibited peaks at 1126, 1035, and 748 cm^{-1} that are attributed to the typical stretching of the cyclic oxetane groups (Figure 1).

After heating at 140 °C for 30 min accompanied with exposure to UV light for 40 s, these characteristic bands disappear completely, which is indicative of the occurrence of cross-linking of the oxetane groups. These results reveal that when the temperature is above the T_g of PCBOD, the two arms of the dendron provide adequate flexibility for the oxetane groups to react in the solid state. In this study, we chose TiO_x to act as hole-blocking and electron-selective layer in the inverted solar cells due to its high electron mobility as well as suitable lowest unoccupied molecular orbital (LUMO = −4.4 eV) and highest occupied molecular orbital (HOMO = −7.6 eV). The TiO_x nanoparticles were first prepared on the indium tin oxide (ITO)

Scheme 1. Synthetic Route for PCBOD and PCBO and Chemical Structure of C-PCBOD

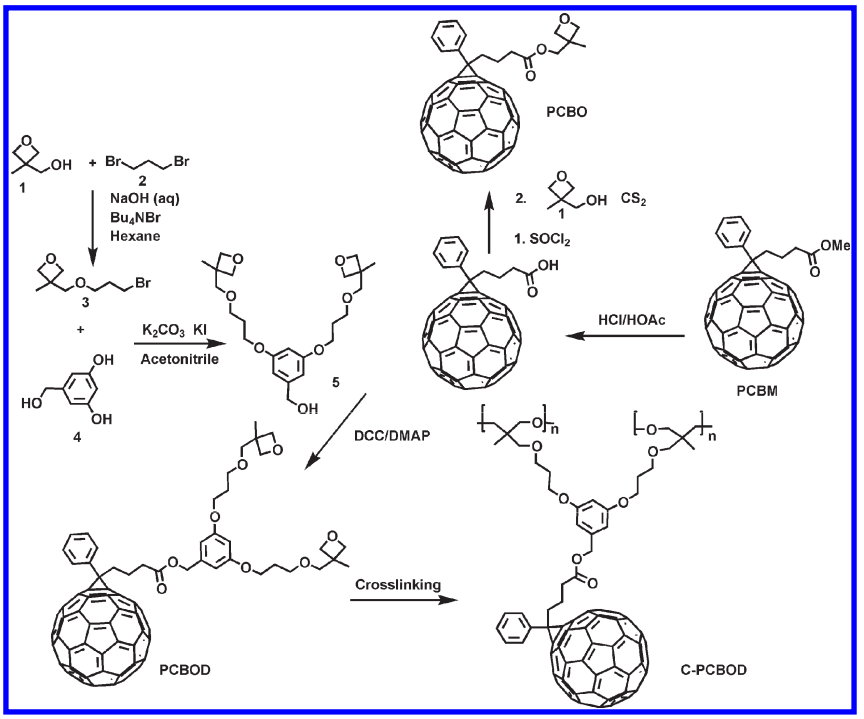

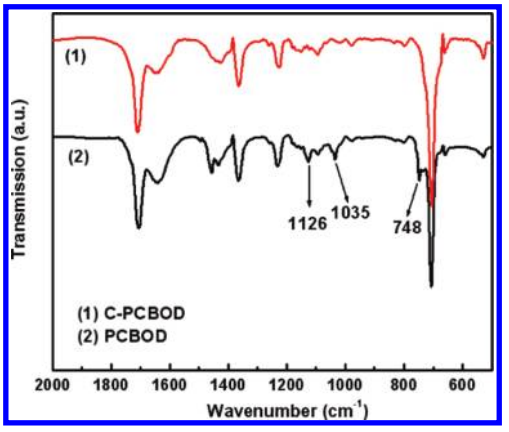

Figure 1. Infrared spectra of the PCBOD precursor and cross-linked PCBOD thin film.

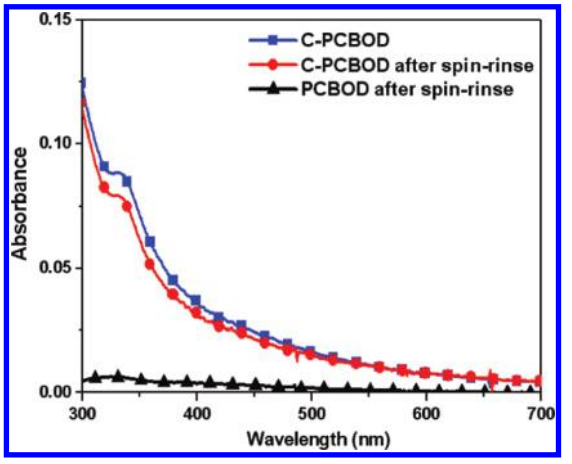

Figure 2. Absorption spectra of cross-linked PCBOD, (■) before and (●) after rinsing with dichlorobenzene, and non-cross-linked PCBOD layer, (▲) after a rinse with dichlorobenzene.

substrate according to the literature.[16] A solution of PCBOD was spin-cast on top of the surface of ITO/TiO_x followed by UV treatment and thermal curing to trigger and facilitate the cross-linking reaction. Contact angle measurement was used to monitor the surface alteration. The bare surface of ITO/TiO_x exhibited a contact angle of ca. 30°. After formation of a cross-linked network of PCBOD on the TiO_x, the wetting contact angle to deionized (DI) water increased to 60° as a result of the increasing hydrophobicity. Most importantly, this cross-linked network produced a robust and adhesive thin film with strong solvent resistance, evidenced by the almost unchanged absorption spectra measured before and after rinsing with *o*-dichlorobenzene (ODCB) (Figure 2). Note that the absorption intensity of the non-cross-linked layer is completely gone after rinsing with ODCB, indicating that, without curing, this thin layer can be totally washed out by the solvent used in the following spin-coating.

Since PCBOD forms a cross-linked network on TiO_x, whether PCBOD molecule can generate chemical bonding at the TiO_x interface is uncertain. To tackle this problem with simplicity, PCBO functionalized with only one oxetane group was employed to specifically evaluate the self-assembly property. Again, a solution of PCBO with a catalytic amount of PAG was spin-coated on top of the surface of ITO/TiO_x, followed by UV irradiation and thermal treatment. Before measurement of the contact angle, the substrate was first rinsed by tetrahydrofuran (THF) to wash away any unbound molecules and then immersed into a THF bath in the ultrasonic cleaner to detach any physically

dx.doi.org/10.1021/cm1032404 |*Chem. Mater.* 2011, 23, 1512–1518

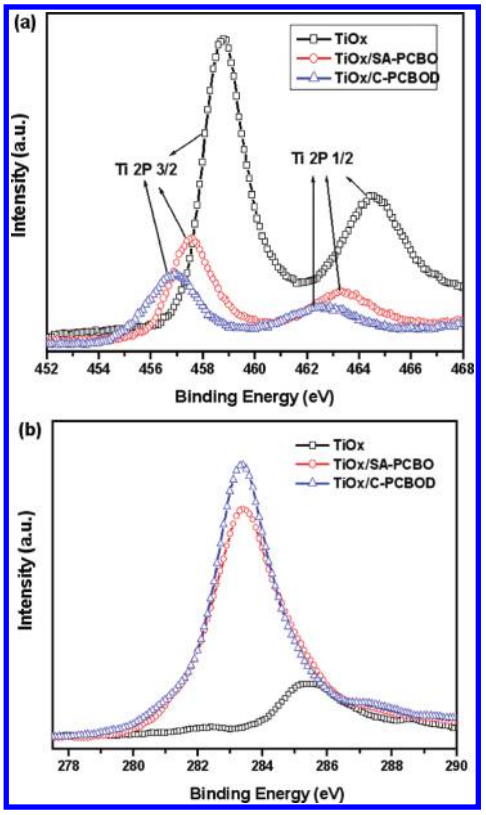

Figure 3. XPS analysis for the ITO/TiO_x, ITO/TiO_x/SA-PCBO, and ITO/TiO_x/C-PCBOD surfaces: (a) titanium 2P and (b) carbon 1S core-level spectra.

adsorbed molecules. The contact angle increased from 30° for the pristine surface to 58° for the modified surface, meaning that the PCBO is indeed attached on the surface. This result indicates that the oxetane functionality in the PCBO molecule must self-assemble on the surface via chemical anchoring. For comparison, we also used a PCBM solution to carry out a control experiment under identical conditions. The contact angle of ITO/TiO_x surface remains essentially unchanged (30°) before and after the modification with PCBM, clearly indicating that PCBM molecules without the oxetane functional group cannot form the chemisorptive binding on the TiO_x surface and thus were completely removed by rinsing and sonication. For a more detailed analysis of the chemical interactions, the surfaces were characterized by X-ray photoelectron spectroscopy (XPS). Figure 3 shows (a) titanium 2P and (b) carbon 1S core-level spectra. The pristine TiO_x surface exhibited a Ti $2P_{3/2}$ peak centered at 458.8 eV and a Ti $2P_{1/2}$ peak centered at 464.5 eV, which are ascribed to Ti^{4+} bond to oxygen, whereas the TiO_x sample modified with the PCBO monolayer showed two peaks at 457.6 and 463.3 eV, respectively. The shifting to the lower binding energy may be associated with the higher negative charge density on Ti due to the chemical modification. Moreover, when the TiO_x modified with a denser cross-linked PCBOD multimolecular layer, the two peaks further shifted to the lower binding energy of 456.9 and 462.9 eV. Also note that there is an obvious decrease in both the Ti $2P_{3/2}$ and Ti $2P_{1/2}$ intensity as the capping layer coverage increases. In addition, we also observed a strong C 1S signal at 283.4 eV with a satellite peak at ~287 eV from both the surfaces of ITO/TiO_x/self-assembled PCBO (SA-PCBO) and ITO/TiO_x/C-PCBOD. However, these fullerene characteristic peaks are not observed for the ITO/TiO_x surface. A small peak showing at ~285.5 eV in the ITO/TiO_x surface may be ascribed to carbon contamination during the film preparation. These XPS results unambiguously confirm the existence of fullerene derivatives on the surfaces.

As can be seen in Figure 4, we propose a mechanism for the self-assembled monolayer and cross-linking of PCBOD on the TiO_x surface.[17] The anchoring of oxetane groups may take place by nucleophilic attack of the hydroxyl groups on the TiO_x surface to open the protonated oxetane rings. Further bidentate anchoring is possible through the etherification condensation. Once the self-assembled monolayer is formed, the intermolecular cross-linking can efficiently occur through ring-opening polymerization between the oxetane groups to vertically grow a multimolecular interlayer.

After demonstrating the SAM properties of PCBO and PCBOD on TiO_x surface, we fabricated an inverted solar cell device B based on the configuration ITO/TiO_x/SA-PCBO/P3HT:PCBM(1:1, w/w)/MoO_3/Ag. The formation of a SAM of PCBO on top of the TiO_x surface allows the deposition of a P3HT:PCBM active layer on top of this modifier without causing interfacial erosion. The following hole-extracting buffer MoO_3 and the silver anode were sequentially deposited by the thermal vacuum evaporation.[18] Under the same condition, a reference device A [ITO/TiO_x/P3HT:PCBM(1:1, w/w)/MoO_3/Ag] without the PCBO modifier was also fabricated for comparison. The $J-V$ characteristics of these devices are shown in Figure 5a and summarized in Table 1. Under AM 1.5G illumination at 100 mW/cm^2, the reference device A showed V_{oc} = 0.58 V, J_{sc} = 10.65 mA/cm^2, FF = 57.8%, and PCE = 3.57%, whereas device B exhibited an overall improvement in the device parameters with V_{oc} = 0.60 V, J_{sc} = 11.14 mA/cm^2, FF = 61%, and PCE = 4.06%. The corresponding external quantum efficiency (EQE) spectra of the devices are also shown in Figure 5b.

This PCE represents a 14% improvement over the unmodified device A. SA-PCBO exerts multiple positive effects in improving the electron-transporting characteristics at the upper and lower interfaces. For the upper contact, compared to the inorganic—organic TiO_x/P3HT:PCBM interface in device A, the organic—organic PCBO/P3HT:PCBM interface with more compatible chemical interaction in device B enhances the electrical coupling and lowers the contact resistance, which facilitates the electron transport and thereby reduces the charge recombination losses at this interface. For the lower contact, the formation of SAM modifier in device B not only forms a more intimate contact to facilitate the electron transport but also terminates the hydroxyl groups on the TiO_x surface to passivate the surface traps. Energetically, SA-PCBO provides an extra P3HT/PCBO interface area for exciton dissociation and serves as an energy gradient intermediate for favorable electron transport. Although the SA-PCBO modifier already improves the device performance to some extent, further improvement in surface modification is possible and desirable. Incomplete coverage of SAM on TiO_x surface results in localized defects where the unmodified TiO_x area is exposed to the upper active layer. Such a contact will lessen the function of the fullerene modifier and have a detrimental effect on the device characteristics. By incorporating a multimolecular cross-linked interlayer, C-PCBOD, to replace the SA-PCBO modifier, we fabricated a device C [ITO/TiO_x/C-PCBOD/P3HT:PCBM(1:1, w/w)/MoO_3/Ag] under similar conditions. Since the two oxetane groups in PCBOD can serve the dual proposes of self-assembly and cross-linking, this

dx.doi.org/10.1021/cm1032404 |*Chem. Mater.* 2011, 23, 1512–1518

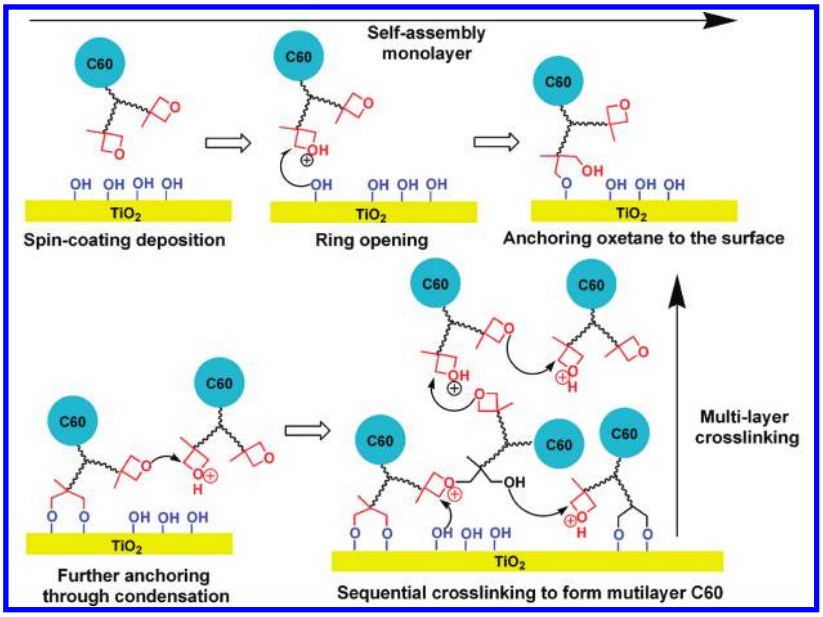

Figure 4. Proposed mechanism for the self-assembly and multimolecular cross-linking of PCBOD on the TiO_x surface.

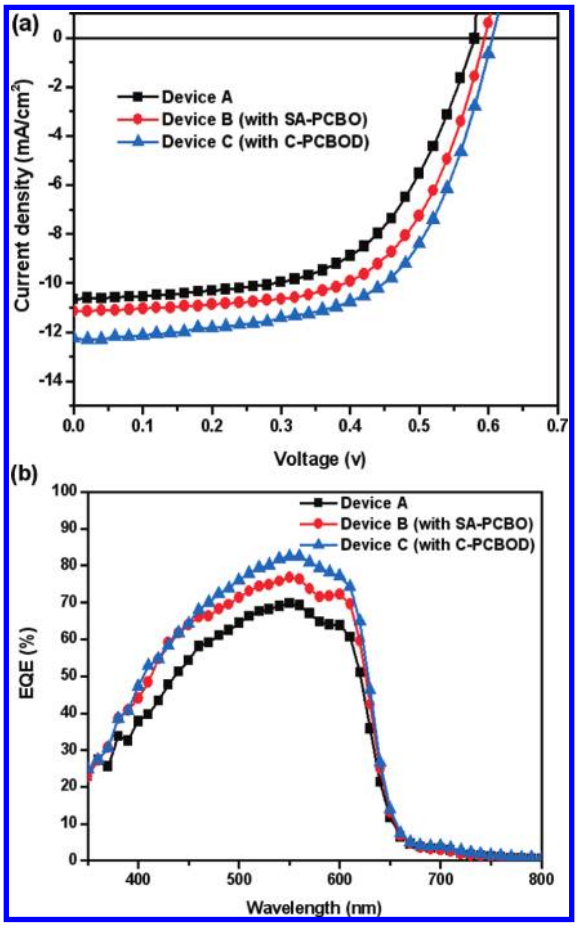

Figure 5. (a) $J-V$ curves of devices A, B, and C under AM 1.5G illumination at 100 mW/cm^2. (b) Corresponding EQE spectra of devices A, B, and C.

interlayer should possess all the aforementioned advantages of the PCBO modifier. The total thickness of the PCBOD interlayer under our processing conditions is ca. 10 nm, which approximately consists of 7−9 layers of PCBOD molecule. The insertion of a dense and robust C-PCBOD interlayer guarantees the PCBSD molecules can completely fill in the voids of the TiO_x surface. Therefore, the upper active layer and the lower TiO_x layer can be fully separated and gradual mutual penetration between the layers in device B can be also avoided. Atomic force microscopy (AFM) was therefore employed to evaluate the surface morphologies of ITO/TiO_x, ITO/TiO_x/SA-PCBO, and ITO/TiO_x/C-PCBSD (Figure 6). The ITO/TiO_x sample shows a very smooth surface with a root-mean-square roughness of 0.48 nm. With a SAM layer of PCBO on the TiO_x, the surface roughness slightly increases to 0.57 nm, with observable pinholes in some localized areas. However, when the surface of ITO/TiO_x is covered by a cross-linked C-PCBOD interlayer, the roughness decreases to 0.43 nm without showing obvious surface defects.

Table 1. Characteristics of Devices A, B, and C

device[a]	V_{oc} (V)	J_{sc} (mA/cm^2)	FF (%)	PCE (%)	R_s	R_{sh}
A	0.58	10.65	57.76	3.57	14.9	465
B	0.60	11.14	60.73	4.06	9.4	588
C	0.61	12.25	61.26	4.50	8.7	625

[a] Device A = ITO/TiO_x/P3HT:PCBM (1:1 w/w)/MoO_3/Ag; device B = ITO/TiOx/SA-PCBO/P3HT:PCBM (1:1 w/w)/MoO_3/Ag; device C = ITO/TiO_x/C-PCBOD/P3HT:PCBM (1:1 w/w)/MoO_3/Ag.

Encouragingly, under AM 1.5G illumination at 100 mW/cm^2, device C exhibited an enhanced V_{oc} of 0.60 V, J_{sc} of 12.25 mA/cm^2, and FF of 61.25%, achieving an exceptional PCE of 4.5%, which is a 10% increase over device B and an overall 26% improvement over device A. This high value is among the best reported for the inverted PSCs.

In conclusion, for the first time, we demonstrate that the oxetane functionality with neutral nature can anchor onto the surface of TiO_x via the facile ring-opening reaction. The self-assembly of PCBO functionalized with one oxetane group on the TiO_x surface not only forms an adhesive monolayer with intimate contact but also passivates the surface electron traps. Device B

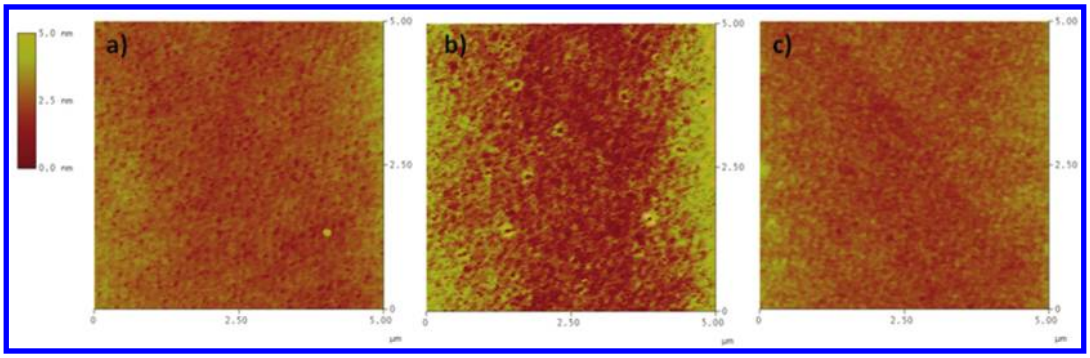

Figure 6. AFM tapping-mode height images of (a) the surface of bare TiO_x, (b) a SA-PCBO on top of the TiO_x, and (c) a C-PCBOD thin film on top of the TiO_x.

with this C_{60} modifier showed a 14% improvement in performance over device A without this monolayer. PCBOD, containing two oxetane groups, is capable of self-assembling on the TiO_x surface and simultaneously undergoing cross-linking, generating a dense, robust, and pinhole-free multimolecular interlayer to further strengthen the interface characteristics. Device C incorporating this interlayer C-PCBOD delivered the best device PCE of 4.5%, which represents 26% enhancement over device A. This high value is among the best reported for P3HT:PCBM-based inverted solar cells. This simple and easy strategy smartly integrates the advantages of self-assembly and cross-linking in a single fullerene-based molecule and shows promise in producing highly efficient inverted PSCs.

EXPERIMENTAL SECTION

General Measurement and Characterization. IR spectra were collected on a PerkinElmer Spectrum One Fourier transform infrared (FT-IR) spectrometer, and the samples were prepared on top of the polished CaF_2 discs for thin-film study. Surface topography was investigated by use of a Veeco Nanoscope 3100 AFM and standard tips (type Tap 300; L, 135 μm; FREQ, 300 MHz; k, 40 N/m). Contact angle measurement was performed with Face Model CAM-Micro by calculating the tangent line of the drop profile. Differential scanning calorimetry (DSC) was measured on TA Q200 Instrument under a nitrogen atmosphere at a heating rate of 10 °C/min. XPS data were measured by Auger Electron Microprobe from VG Scientific Microlab 350.

Device Fabrication. The TiO_x was prepared by a sol−gel procedure from titanium(IV) isopropoxide (TTIP). The solar cell devices were fabricated under optimized conditions according to the following procedure: Indium tin oxide- (ITO-) coated glass substrate was first cleaned with detergent; ultrasonicated in DI water, acetone, and isopropyl alcohol for 10 min, respectively; and subsequently dried in an oven overnight. Nanosized TiO_x thin films with a thickness of ca. 50 nm were prepared by spin-coating the sol−gel precursor solution at 2000 rpm on top of the ITO substrate. The films were heated at 200 °C for 5 min in nitrogen atmosphere and then sintered at 450 °C for 1 h in air. During this process the precursor converts to solid-state TiO_x (i.e., gel of TiO_x) and forms a transparent nanoparticle TiO_x thin film. For devices fabricated with a C-PCBOD interlayer, an *o*-DCB solution containing PCBOD and diphenyliodonium hexafluoroarsenate (6 wt % to PCBOD) was spin-cast on the TiO_x film to form a thin film with a thickness of ca. 10 nm. Subsequently, the as-cast film was heated at 140 °C for 30 min and UV treatment for 40 s in the glovebox for cross-linking. For devices fabricated with a self-assembled PCBO monolayer, an *o*-DCB solution containing PCBO and the photoacid generator (6 wt % to PCBO) was spin-cast on the TiO_x film to form a thin film. Subsequently, the as-cast film was heated at 140 °C for 30 min and UV-treated for 40 s in the glovebox. The samples were then sonicated in THF solution for 1 min to remove any physically absorbed SAM molecules. For devices A, B, and C, *o*-DCB solution containing a mixture of P3HT/$PC_{61}BM$ (1:1, w/w) was then spin-cast to form a 250-nm thin film on top of the TiO_x, SA-PCBO, and C-PCBOD thin films, respectively. After thermal annealing at 140 °C for 15 min in the glovebox, the MoO_3 layer (7 nm) was evaporated thermally at a pressure below 10^{-6}. Finally, the top electrode, made of Ag film (100 nm thick), was evaporated thermally at a pressure below 10^{-6} Torr. The devices without encapsulation were characterized in the ambient condition. Current−voltage characteristics were measured on a Keithley 2400 SMU under the irradiation of AM 1.5G San-Yi solar simulator with JIS AAA spectrum. The characteristics of the solar cells were optimized by testing approximately 50 cells.

3-[(3-Bromopropoxy)methyl]-3-methyloxetane (3). To a solution of sodium hydroxide (65.0 g, 1.625 mol) in water (100 mL) were added 3-methyl-3-oxetanemethanol **1** (10 g, 0.098 mol), 1,3-dibromopropane **2** (59.3 g, 0.294 mol), tetrabutylammonium bromide (0.5 g), and hexane (100 mL). The mixture was stirred for 24 h at room temperature and then refluxed for 30 min. After the solution was cooled to room temperature, water (100 mL) was added to the solution. The solution was extracted with hexane (100 mL × 3), and water (150 mL × 2). The combined organic layer was dried over $MgSO_4$. After removal of the solvent under reduced pressure, the residue was purified by distillation under reduced pressure (0.18 Torr, 80 °C) to get colorless liquid **3** (12 g, 55%). ^{1}H NMR (300 MHz, $CDCl_3$, δ): 1.30 (s, 3H), 2.07−2.15 (m, 2H), 3.46 (s, 2H), 3.51 (t, 2H, J = 6 Hz), 3.59 (t, 2H, J = 6 Hz), 4.34 (d, 2H, J = 5.7 Hz), 4.50 (d, 2H, J = 5.7 Hz). ^{13}C NMR (75 MHz, $CDCl_3$, δ): 21.3, 30.6, 32.6, 39.9, 68.6, 76.2, 80.0, 80.1.

{3,5-Bis{3-[(3-methyloxetan-3-yl)methoxy]propoxy}phenyl}methanol (5). A solution of 3,5-dihydroxybenzyl alcohol **4** (0.2 g, 1.43 mmol) and K_2CO_3 (1.18 g, 8.54 mmol) in acetonitrile (25 mL) was refluxed for 1 h, and then compound **3** (0.7 g, 3.14 mmol), and a trace amount of KI were added. The solution was then refluxed for 24 h. After the solution was cooled to room temperature, the white solid was filtered off and the filtrate was extracted by ethyl acetate. After removal of the solvent under reduced pressure, the residue was purified by column chromatography on silica gel (hexane/ethyl acetate, 2/1 v/v) to give a brown oil **5** (0.42 g, 69%). ^{1}H NMR (300 MHz, $CDCl_3$, δ): 1.28 (s, 6H), 2.00−2.26 (m, 4H), 2.26 (s, 1H), 3.47 (s, 4H), 3.73 (t, 4H, J = 6 Hz), 4.09 (t, 4H, J = 6 Hz), 4.33 (d, 4H, J = 5.7 Hz), 4.50 (d, 4H, J = 5.7 Hz), 4.59 (s, 2H), 6.37 (s, 1H), 6.51 (s, 2H). ^{13}C NMR (75 MHz, $CDCl_3$, δ): 21.3, 29.5, 39.8, 64.8, 65.2, 67.8, 76.0, 80.1, 100.6, 105.1, 143.5, 160.3. EI-MS [m/z (%)]: calcd for $C_{23}H_{36}O_7$, 424.53; found, 424.

[6,6]-Phenyl-C_{61}-butyric Oxetane Dendron Ester (PCBOD). To a solution of PCBA (0.1 g, 0.11 mmol), **5** (0.043 g, 0.1 mmol), and 4-(dimethylamino)pyridine (0.014 g, 0.11 mmol) in 1,2-dichlorobenzene (40 mL) was added *N,N′*-dicyclohexylcarbodiimide

(0.023 g, 0.11 mmol) at 0 °C. The solution was then stirred at room temperature for 24 h. After removal of the solvent under reduced pressure, the residue was purified by silica gel chromatography with toluene/ethyl acetate (10/1 v/v) as the eluent. The product was redissolved in toluene and precipitated out by adding the solution into methanol (250 mL) to give a brown solid, PCBOD (0.1 g, 76%). ^{1}H NMR (300 MHz, $CDCl_3$, δ): 1.30 (s, 1H), 2.0−2.09 (m, 4H), 2.17−2.23 (m, 2H), 2.58 (t, 2H, J = 7.4 Hz), 2.92 (t, 2H, J = 8.3 Hz), 3.49 (s, 4H), 3.64 (t, 4H, J = 6 Hz), 4.03 (t, 4H, J = 6 Hz), 4.34 (d, 4H, J = 5.7 Hz), 4.50 (d, 4 H, J = 5.7 Hz), 5.03 (s, 2H), 6.39 (s, 1H), 6.47 (s, 2H), 7.47−7.56 (m, 3H), 7.92 (d, 2H, J = 9 Hz). ^{13}C NMR (125 MHz, $CDCl_3$, δ): 21.4, 22.3, 29.6, 29.7, 33.6, 34.0, 39.9, 51.8, 64.9, 66.3, 67.9, 76.2, 79.9, 80.1, 101.0, 106.6, 128.3, 128.4, 132.1, 136.7, 137.6, 138.0, 138.1, 140.7, 141.0, 142.09, 142.1, 142.17, 142.2, 142.9, 142.93, 142.96, 143.0, 143.04, 143.7, 143.75, 144.0, 144.4, 144.5, 144.65, 144.7, 144.8, 145.0, 145.07, 145.12, 145.2, 145.8, 147.8, 148.8, 160.3, 172.8.

[6,6]-Phenyl-C_{61}-butyric Oxetane Ester (PCBO). To a suspension of PCBA (115 mg, 0.132 mmol) in dry carbon disulfide (37 mL) under nitrogen was added thionyl chloride (37 mL) at room temperature. The resulting mixture was heated at reflux for 18 h and the volatile components were removed on a rotary evaporator. To the residue were added dry toluene (12.5 mL), pyridine (0.5 mL), and then 3-methyl-3-oxetanemethanol **1** (33 mg, 0.32 mmol). The reaction was stirred at room temperature for 20 h and the solvent was removed. The residue was purified by column chromatography on silica gel (hexane/ethyl acetate, 10/1 v/v) to give a brown powder, PCBO (59 mg, 46%); mp 142 °C. ^{1}H NMR ($CDCl_3$, 300 MHz, δ): 1.31 (s, 3H), 2.18−2.24 (m, 2H), 2.58 (t, 2H, J = 7.5 Hz), 2.89−2.95 (m, 2H), 4.17 (s, 2H), 4.37 (d, 2H, J = 6.0 Hz), 4.39 (d, 2H, J = 6.0 Hz), 7.47−7.58 (m, 3H), 7.93 (d, 2H, J = 9.0 Hz); ^{13}C NMR ($CDCl_3$, 75 MHz, δ): 21.2, 22.4, 33.6, 34.0, 39.0, 51.8, 68.7, 79.5, 79.8, 128.3, 128.4, 132.1, 136.7, 137.6, 138.0, 140.7, 141.0, 142.1, 142.16, 142.2, 142.9, 142.98, 143.0, 143.1, 143.7, 144.0, 144.4, 144.5, 144.7, 144.8, 145.0, 145.1, 145.2, 145.8, 147.7, 148.7, 173.1. Anal. calcd for $C_{76}H_{20}O_3$: C 77.48, H 10.28. Found: C 77.81, H 9.65.

■ ASSOCIATED CONTENT

Ⓢ Supporting Information. TGA, DSC, CV, contact angle measurements, and NMR spectra of the new compounds. This material is available free of charge via the Internet at http://pubs.acs.org.

■ AUTHOR INFORMATION

Corresponding Author
*E-mail yjcheng@mail.nctu.edu.tw.

■ ACKNOWLEDGMENT

This work was supported by the National Science Council and "ATU Plan" of the National Chiao Tung University and Ministry of Education, Taiwan.

■ REFERENCES

(1) (a) Yu, G.; Gao, J.; Hummelen, J. C.; Wudl, F.; Heeger, A. J. *Science* **1995**, *270*, 1789. (b) Thompson, B. C.; Frechet, J. M. J. *Angew. Chem., Int. Ed.* **2008**, *47*, 58. (c) Günes, S.; Neugebauer, H.; Sariciftci, N. S. *Chem. Rev.* **2007**, *107*, 1324. (d) Cheng, Y. J.; Yang, S. H.; Hsu, C. S. *Chem. Rev.* **2009**, *109*, 5868.

(2) (a) Woo, C. H.; Thompson, B. C.; Kim, B. J.; Toney, M. F.; Frechet, J. M. J. *J. Am. Chem. Soc.* **2008**, *130*, 16324. (b) Reyes-Reyes, M.; Kim, K.; Carroll, D. L. *Appl. Phys. Lett.* **2005**, *87*, No. 083506. (c) Li, G.; Shrotriya, V.; Huang, J.; Yao, Y.; Moriarty, T.; Emery, K.; Yang, Y. *Nat. Mater.* **2005**, *4*, 864. (d) Ma, W.; Yang, C.; Gong, X.; Lee, K.; Heeger, A. J. *Adv. Funct. Mater.* **2005**, *15*, 1617.

(3) (a) Li, G.; Chu, C. W.; Shrotriya, V.; Huang, J.; Yang, Y. *Appl. Phys. Lett.* **2006**, *88*, No. 253503. (b) Liao, H. H.; Chen, L. M.; Xu, Z.; Li, G.; Yang, Y. *Appl. Phys. Lett.* **2008**, *92*, No. 173303.

(4) (a) Mor, G. K.; Shankar, K.; Paulose, M.; Varghese, O. K.; Grimes, C. A. *Appl. Phys. Lett.* **2007**, *91*, No. 152111. (b) Waldauf, C.; Morana, M.; Denk, P.; Schilinsky, P.; Coakley, K.; Choulis, S. A.; Brabec, C. J. *Appl. Phys. Lett.* **2006**, *89*, No. 233517. (c) White, M. S.; Olson, D. C.; Shaheen, S. E.; Kopidakis, N.; Ginley, D. S. *Appl. Phys. Lett.* **2006**, *89*, No. 143517. (d) Steim, R.; Choulis, S. A.; Schilinsky, P.; Brabec, C. J. *Appl. Phys. Lett.* **2008**, *92*, No. 093303. (e) Wang, T.; Cai, W.; Qin, D.; Wang, E.; Lan, L.; Gong, X.; Peng, J.; Cao, Y. *J. Phys. Chem. C* **2010**, *114*, 6849.

(5) (a) Lee, S.; Koo, B.; Shin, J.; Lee, E.; Park, H.; Kim, H. *Appl. Phys. Lett.* **2006**, *88*, No. 162109. (b) McDowell, M.; Hill, I. G.; McDermott, J. E.; Bernasek, S. L.; Schwartz, J. *Appl. Phys. Lett.* **2006**, *89*, No. 073505. (c) Chua, L. L.; Zaumseil, J.; Chang, J. F.; Ou, E. C. W.; Ho, P. K. H.; Sirringhaus, H.; Friend, R. H. *Nature* **2005**, *434*, 194.

(6) Wei, Q.; Nishizawa, T.; Tajima, K.; Hashimoto, K. *Adv. Mater.* **2008**, *20*, 2211.

(7) (a) Liang, C. W.; Su, W. F.; Wang, L. *Appl. Phys. Lett.* **2009**, *95*, No. 133303. (b) Huang, J. S.; Chou, C. Y.; Lin, C. F. *Sol. Energy Mater. Sol. Cells* **2010**, *94*, 182.

(8) (a) Hau, S. K.; Yip, H. L.; Baek, N. S.; Zou, J.; O'Malley, K.; Jen, A. K. Y. *Appl. Phys. Lett.* **2008**, *92*, No. 253301. (b) Hau, S. K.; Yip, H. L.; Acton, O.; Baek, N. S.; Ma, H.; Jen, A. K. Y. *J. Mater. Chem.* **2008**, *18*, 5113. (c) Hau, S. K.; Yip, H. L.; Ma, H.; Jen, A. K. Y. *Appl. Phys. Lett.* **2008**, *93*, No. 233304.

(9) Goh, C.; Scully, S. R.; McGehee, M. D. *J. Appl. Phys.* **2007**, *101*, No. 114503.

(10) (a) Chou, T. P.; Zhang, Q.; Cao, G. *J. Phys. Chem. C* **2007**, *111*, 18804.

(11) (a) Hsieh, C.-H.; Cheng, Y.-J.; Li, P.-J.; Chen, C.-H.; Dubosc, M.; Liang, R.-M.; Hsu, C.-S. *J. Am. Chem. Soc.* **2010**, *132*, 4887. (b) Cheng, Y.-J.; Hsieh, C.-H.; He, Y.; Hsu, C.-S.; Li, Y. *J. Am. Chem. Soc.* **2010**, *132*, 17381.

(12) Veinot, J. G. C.; Marks., T. J. *Acc. Chem. Res.* **2005**, *38*, 632 and references therein.

(13) (a) Huang, F.; Cheng, Y.-J.; Zhang, Y.; Liu, M. S.; Jen, A. K.-Y. *J. Mater. Chem.* **2008**, *18*, 4485. (b) Müller, D. C.; Falcou, A.; Reckefuss, N.; Rojahn, M.; Wiederhirn, V.; Rudati, P.; Frohne, H.; Nuyken, O.; Becker, H.; Meerholz, K. *Nature* **2003**, *421*, 829. (c) Bacher, E.; Bayerl, M.; Rudati, P.; Reckefuss, N.; Müller, C. D.; Meerholz, K.; Nuyken, O. *Macromolecules* **2005**, *38*, 1640. (d) Gather, M. C.; Köhnen, A.; Falcou, A.; Becker, H.; Meerholz, K. *Adv. Funct. Mater.* **2007**, *17*, 191. (e) Zacharias, P.; Gather, M. C.; Rojahn, M.; Nuyken, O.; Meerholz, K. *Angew. Chem., Int. Ed.* **2007**, *46*, 4388.

(14) Goncalves, R. H.; Schreiner, W. H.; Leite, E. R. *Langmuir* **2010**, *26*, 11657.

(15) Hau, S. K.; Cheng, Y.-J.; Yip, H.-L.; Zhang, Y.; Ma, H.; Jen, A. K.-Y. *ACS Appl. Mater. Interfaces* **2010**, *2*, 1892.

(16) Cho, S.; Lee, K.; Heeger., A. J. *Adv. Mater.* **2009**, *21*, 1.

(17) Köhen, A.; Riegel, N.; Kremer, J. H.-W. M.; Lademann, H.; Müller, D. C.; Meerholz, K. *Adv. Mater.* **2009**, *21*, 879.

(18) (a) Tao, C.; Ruan, S.; Zhang, X.; Xie, G.; Shen, L.; Kong, X.; Dong, W.; Liu, C.; Chen, W. *Appl. Phys. Lett.* **2008**, *93*, No. 193307. (b) Kyaw, A. K. K.; Sun, X. W.; Jiang, C. Y.; Lo, G. Q.; Zhao, D. W.; Kwong, D. L. *Appl. Phys. Lett.* **2008**, *93*, No. 221107.